Journal of Civil Engineering and Urban Planning (2025)
Clausius Scientific Press, Canada

DOI: 10.23977/jceup.2025.070206
ISSN 2616-3969 Vol. 7 Num. 2

Calculation Method of Pile Foundation Deformation under the Coupled Action of Bank Slope Siltation and Creep

Liangwei Sun[1], Chao Liang[1,a,*]

[1]*State Key Laboratory of Hydraulic Engineering Intelligent Construction and Operation, Tianjin University, Tianjin, China*
[a]*liangchao@tju.edu.cn*
**Corresponding author*

Keywords: Creep, Bank Slope Siltation, Pile Foundation Deformation, *P-Y* Curve

Abstract: Soil creep is the process where soil deformation progressively increases under sustained loading. Under the coupled action of berth siltation soil and berth loads, soil creep occurs, impacting pile foundation bearing capacity. This paper investigates the creep characteristics of various soils, analyzes how soil strength and deformation affect pile foundation load response, and revises the *p-y* curve method for creep conditions. The results show that under the coupled action of bank slope siltation and creep, the long-term soil strength declines. The ε_{50} value, which is the strain at half the maximum principal stress difference in isochronous curves, gradually increases. The horizontal pile displacement becomes larger, yet with increasing time, the incremental horizontal displacement of the pile foundation becomes smaller and smaller.

1. Introduction

As a common foundation type for docks, single-pile foundations are characterized by low self-weight, simple structure, and clear stress distribution[1]. Soil creep caused by the coupled action of dock loads and silt changes soil strength and deformation, affecting pile foundation bearing capacity.

Yang(2022)[2], via 1D consolidation creep tests, found that remolded soft clay undergoes significant instantaneous deformation during creep, with slow, gradual deformation reduction toward stabilization as loading time increases. Zhou(2006)[3] conducted a series of triaxial tests to explore how factors like soil's initial consolidation degree, drainage conditions, and load ratio affect soft soil creep. Hu(2023)[4], with triaxial shear creep tests, observed strain-hardening in remolded overconsolidated saturated clay, noting earlier creep onset and smaller creep deformation with higher overconsolidation ratios. Long(2010)[5] divided the creep process into three stages: steady-state creep, accelerating creep, and creep failure, based on triaxial and direct shear creep tests. These studies focused on analyzing soft soil creep via indoor tests but did not deeply explore the impact of soil creep on foundation horizontal bearing capacity. The *p-y* curve method recommended by API(2014)[6] also does not account for soil creep effects on pile foundation capacity.

This paper analyzes the creep characteristics of different soils to study their effect on pile

foundation bearing capacity. It first examines how soil creep influences the strain value ε_{50} at half the maximum principal stress difference in isochronous curves. Then, it revises the *p-y* curve method and uses numerical analysis to simulate the impact of soil creep on pile foundation capacity.

2. Impact of Soil Creep on *p-y* Curves

2.1. Calculation Method of *p-y* Curves for Clay

Use the *p-y* curve method from API(2014)[6] to calculate horizontal load responses of pile foundations. The detailed calculation method is shown in equations (1)~(4) and Table 1.

$$\text{For } 0<z\le z_R, \qquad p_u D = 3s_u D + \gamma' zD + Js_u z \tag{1}$$

$$\text{For } z\ge z_R, \qquad p_u D = 9s_u D \tag{2}$$

$$z_R = \frac{6D}{\frac{\gamma' D}{s_u} + J} \tag{3}$$

$$y_c = 2.5 \times \varepsilon_{50} \times D \tag{4}$$

Table 1 Horizontal resistance-displacement data

p/p_u	0.00	0.23	0.33	0.50	0.72	1.00	1.00
y/y_c	0.0	0.1	0.3	1.0	3.0	8.0	∞

p_uD represents ultimate resistance per unit length (N/m), p_u the ultimate resistance (N), s_u the soil's undrained shear strength (kPa), D the pile diameter (m), γ' the soil effective unit weight (kN/m^3), J a dimensionless constant, z the depth below the mudline, z_R the depth from the mudline to the bottom of the soil resistance reduction zone (m), and y the horizontal pile displacement.

2.2. Creep Test Analysis

By analyzing the creep tests done by scholars [7-13], this paper studies the impact of soil creep on ε_{50} in the *p-y* curve method. The soil parameters are shown in Table 2.

Table 2 Basic physical and mechanical parameters of soil

Soil	Zhuhai[7]	Zhangzhou[8]	Binhai[9]	Shantou[10]	Wangjiang[11]	Wenzhou[12]	Shanghai[13]
I_P	37.2	35.8	20.38	16	17.3	23.1	15.4
c/kPa	4.6	8	15	15.9	15.4	9.8	16.7

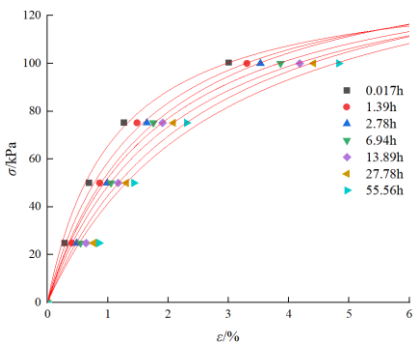

Figure 1 Stress-strain isochronous curve

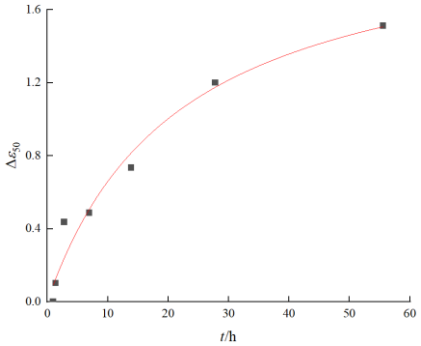

Figure 2 The curve of Δε50-t

Take the triaxial consolidation undrained shear creep test of Zhuhai soft soil at 100kPa cell pressure[7] as an example to analyze the variation of ε_{50} during soil creep. The stress-strain isochronous curves are shown in Figure 1, and the variation of the strain growth value $\Delta\varepsilon_{50}$ at half the maximum principal stress difference with time is shown in Figure 2.

From Figure 1, the initial elastic modulus of soil decreases and its long-term strength drops gradually during creep. Figure 2 shows that ε_{50} increases gradually with time.

2.3. Modified *p-y* Curves for Clay

The relationship curve between the normalized strain value at half the maximum principal stress difference for different soils $\Delta\varepsilon_{50}(t)/\Delta\varepsilon_{50}(t=0\text{h})$ and the plasticity index I_p at the same time is shown in Figure 3 (taking t=24h as an example).

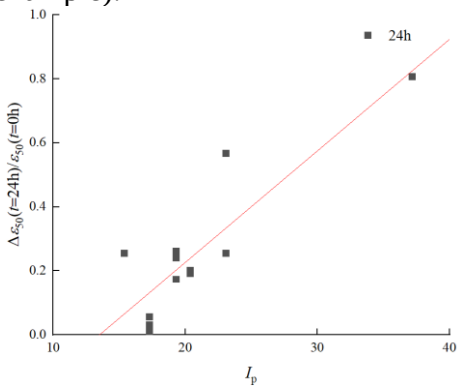

Figure 3 The curve of Δε50(t=24h)/Δε50(t=0h)-Ip

From Figure 3, $\Delta\varepsilon_{50}(t)/\Delta\varepsilon_{50}(t=0\text{h})$ increases with I_p. A fitting of the $\Delta\varepsilon_{50}(t=24\text{h})/\Delta\ \varepsilon_{50}(\text{t=0h})$-$I_p$ curve in Figure 3 yields equation (5).

$$\frac{\Delta\varepsilon_{50}(t)}{\Delta\varepsilon_{50}(t=0\text{h})} = 0.03488\times I_p - 0.47174 \tag{5}$$

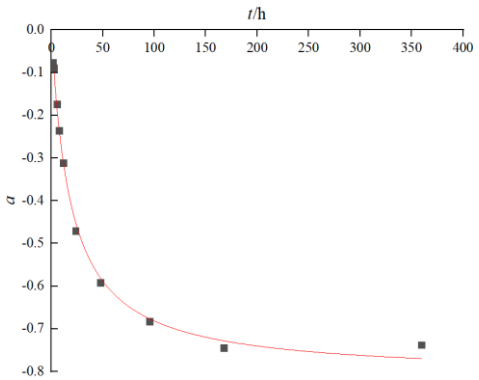

Figure 4 Coefficient a-t curve

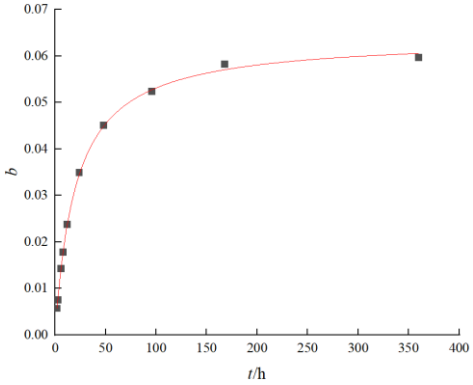

Figure 5 Coefficient b-t curve

Equations (6)~(8) provide a method to calculate ε_{50} during soil creep, thus revising the *p-y* curve method recommended by the API specification[6].

The relationship between $\Delta\varepsilon_{50}(t)/\Delta\varepsilon_{50}(t=0\text{h})$ and I_p at different times is expressed by equation (6). The relationship between coefficients a, b and t is shown in Figures 4 and 5. a and b are fitting coefficients. The relationship curves between coefficients a, b and time in Figures 4 and 5 are fitted to obtain equations (7) and (8).

$$\frac{\Delta\varepsilon_{50}(t)}{\Delta\varepsilon_{50}(t=0\text{h})} = a + b \times I_{\text{p}} \tag{6}$$

$$a = \frac{-t}{23.26 + 1.23 \times t} \tag{7}$$

$$b = \frac{t}{319.73 + 15.62 \times t} \tag{8}$$

3. Pile Load Response under Bank Slope Siltation and Creep Coupling

3.1. Numerical Model Establishment

Numerical analysis on the horizontal load response of pile foundations under the coupled action of bank slope siltation and creep was carried out using the ABAQUS finite element software.A 42m-long pile with a 0.75m diameter and 38m burial depth was modeled. Soil layers were set every 2m below the mudline, with a soil spring applied at the midpoint of each layer and creep parameters input at connection sections. The soil's plasticity index I_{p} was 20, with undrained shear strength s_{u} increasing linearly from 50kPa at the first layer to s_{u} =50+1.2z with depth z. The effective unit weight of the soil was 8.5kN/m ³A horizontal load F_1 was applied at the pile head to simulate the dock load, and another load F_2 at 2.67m below the mudline to simulate the effect of siltation on the pile foundation. p-y curves at different times were input for each soil layer to account for the influence of soil creep on the pile foundation. The loading conditions are shown in Figure 6.

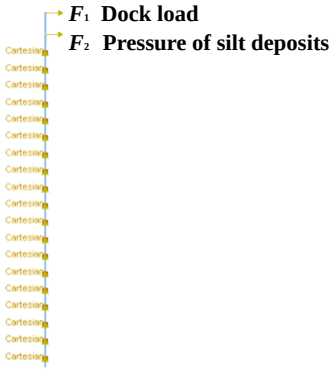

Figure 6 Numerical model

3.2. Pile Load Response Analysis

Zdravkovic(2015)[14] defined the horizontal bearing capacity of pile foundations as the foundation resistance corresponding to a mudline displacement of 0.1D under lateral loading. To more accurately simulate the horizontal load response of pile foundations under the coupled action of bank slope siltation and creep, soil spring models at different creep times were established in ABAQUS. The pile foundation was subjected to dock loads and soil pressure from the siltation, and the load-displacement curves at the pile head, pile depth-displacement curves, and horizontal bearing capacity-time curves are shown in Figures 7,8 and 9.

From Figure 7, under the same lateral load, pile foundation horizontal displacement increases with creep time. The initial displacement growth is rapid but slows to nearly zero. From Figure 8, pile horizontal displacement decreases with depth. A inflection point appears at 12m depth. Above 12m, displacement decreases nearly linearly; below 12m, it approaches zero, indicating fixed ends

at the lower pile and base. From Figure 9, due to soil strength decay with creep time, pile horizontal bearing capacity decreases over time. Most capacity is lost by one month, after which the decay slows.

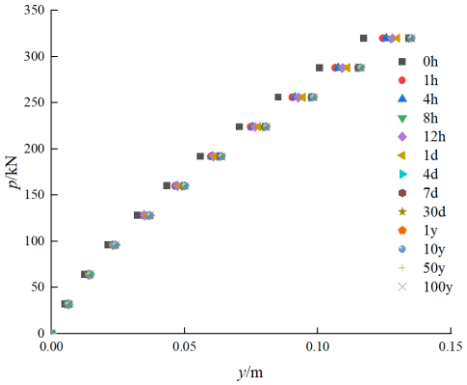

Figure 7 Load-displacement curve

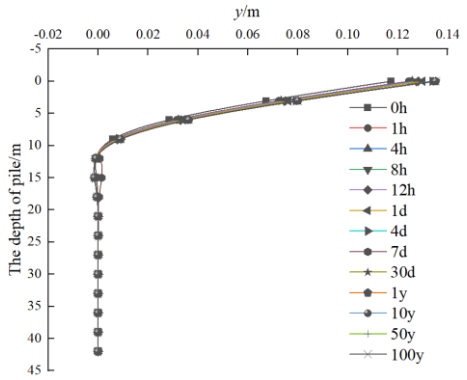

Figure 8 Pile depth-displacement curve

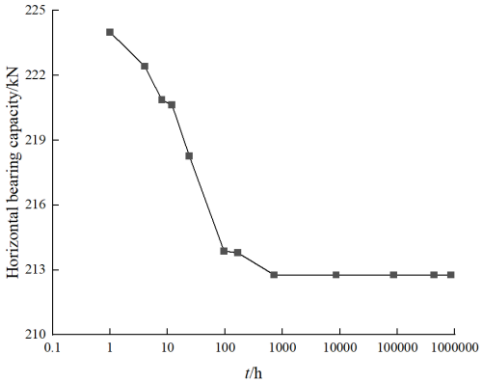

Figure 9 Horizontal bearing capacity-time curve

4. Conclusions

Through simulations using ABAQUS finite element software, the horizontal load response of pile foundations under the coupled action of bank slope siltation and creep was studied. Here are the key findings:

As creep time rises, the soil's initial elastic modulus and long - term strength decrease, while the strain value ε_{50} at half the maximum principal stress difference increases. A modified *p-y* curve method considering soil creep effects is proposed.

Under the coupled action of bank slope siltation and creep, pile foundation horizontal displacement grows with time, but the increment declines. Within a certain pile burial depth range, horizontal displacement diminishes nearly linearly with depth, approaching zero, with fixed ends appearing at the lower part and base of the pile.

As the action time of dock loads and silt pressure on the pile increases, the pile's horizontal bearing capacity decreases. Initially, it drops rapidly; after one month, most of the capacity is lost, and in the later stage, it decays slowly.

Acknowledgements

This research was supported by the Open Fund Project of National Key R&D Program of China (2022YFB2603000).

References

[1] Doherty P, Gavin K. Laterally loaded monopile design for offshore wind farms [J]. Proceedings of the institution of civil engineers-energy, 2012, 165(1): 7-17.

[2] Yang, A. W., Liang, Z. Z., Yang, S. K., et al. One-dimensional Consolidation and Creep Characteristics of Remolded Soft Clay in Tianjin Coastal Area [J]. Chinese Journal of Underground Space and Engineering, 2022, 18(05): 1532-1538.

[3] Zhou, Q. J., Chen, X. P. Experimental Study on Creep Characteristics of Soft Soil [J]. Chinese Journal of Geotechnical Engineering, 2006, (05): 626-630.

[4] Hu, M. Y., Xiao, B., Lu, Y. K., et al. Creep Tests and Models for Remolded Overconsolidated Saturated Clay [J]. Chinese Journal of Geotechnical Engineering, 2023, 45(S1): 6-10.

[5] Long, J. H., Guo, W. B., Li, P., et al. Creep Characteristics of Slip Zone Soil in Loess Landslide [J]. Chinese Journal of Geotechnical Engineering, 2010, 32(07): 1023-1028.

[6] American Petroleum Institute. Geotechnical and foundation design considerations [S]. ANSI/API recommended practice 2GEO first edition, 2014.

[7] Zhu, Q. W. Macroscopic and Microscopic Creep Tests and Nonlinear Model Research on Zhuhai Soft Clay [D]. Guangzhou University, 2020.

[8] Zhang, X. W., Wang, C. M. An Empirical Creep Model for Saturated Soft Clay [J]. Journal of Central South University (Natural Sciences), 2011, 42(03): 791-796.

[9] Li, K. F. Study on the Creep Characteristics of Marine Soft Clay and the Post-Construction Settlement Effect of Roadbeds [D]. Tianjin University, 2018.

[10] Luo, Q. Z., Chen, X. P., Wang, S., et al. Experimental and Empirical Model Study on the Time-Dependent Deformation of Soft Clay [J]. Rock and Soil Mechanics, 2016, 37(01): 66-75.

[11] Yang, C., Dai, G. L., Gong, W. M., et al. Experimental Study on the Creep Characteristics of Typical Silty Clay in Wangjiang Area [J]. China Civil Engineering Journal, 2015, 48(S2): 47-52.

[12] Gao, Z. Analysis of Deep Excavation Deformation Characteristics Considering the Creep Effect of Mud [D]. Yangzhou University, 2021.

[13] Xu, X. B. Study on the Creep Characteristics and Fractional Constitutive Model of Soft Clay [D]. China University of Mining and Technology, 2020.

[14] Zdravkovic L, Taborda D M G, Potts D, et al. Numerical modelling of large diameter piles under lateral loading for offshore wind applications [J]. Frontiers in offshore geotechnics III. 2015, 1: 759-764.